© 2014. Published by The Company of Biologists Ltd | The Journal of Experimental Biology (2014) 217, 261-273 doi:10.1242/jeb.083923

RESEARCH ARTICLE

Comparison of rotator cuff muscle architecture between humans and other selected vertebrate species

Margie A. Mathewson[1], Alan Kwan[2], Carolyn M. Eng[3], Richard L. Lieber[1,4,5] and Samuel R. Ward[1,2,4,*]

ABSTRACT

In this study, we compare rotator cuff muscle architecture of typically used animal models with that of humans and quantify the scaling relationships of these muscles across mammals. The four muscles that correspond to the human rotator cuff – supraspinatus, infraspinatus, subscapularis and teres minor – of 10 commonly studied animals were excised and subjected to a series of comparative measurements. When body mass among animals was regressed against physiological cross-sectional area, muscle mass and normalized fiber length, the confidence intervals suggested geometric scaling but did not exclude other scaling relationships. Based on the architectural difference index (ADI), a combined measure of fiber length-to-moment arm ratio, fiber length-to-muscle length ratio and the fraction of the total rotator cuff physiological cross-sectional area contributed by each muscle, chimpanzees were found to be the most similar to humans (ADI=2.15), followed closely by capuchins (ADI=2.16). Interestingly, of the eight non-primates studied, smaller mammals such as mice, rats and dogs were more similar to humans in architectural parameters compared with larger mammals such as sheep, pigs or cows. The force production versus velocity trade-off (indicated by fiber length-to-moment arm ratio) and the excursion ability (indicated by fiber length-to-muscle length ratio) of humans were also most similar to those of primates, followed by the small mammals. Overall, primates provide the best architectural representation of human muscle architecture. However, based on the muscle architectural parameters of non-primates, smaller rather than larger mammals may be better models for studying muscles related to the human rotator cuff.

KEY WORDS: Architecture, Muscle, Rotator cuff

INTRODUCTION

One of the most common causes of pain and disability in the upper extremity is injury or disease of the shoulder, specifically to the tendons of the rotator cuff muscles. Rotator cuff tendon tears are caused by acute or chronic injuries and appear to degenerate with age. In people under 40 years of age, acute tears are seen more frequently and can be caused by events such as contact sports accidents (Blevins, 1997; Skinner, 2007). Chronic tears are often seen in middle-aged or older athletes or in people who frequently participate in overhand sports activities such as tennis or pitching (Blevins, 1997). Current treatments for rotator cuff injuries vary from conservative physical therapy to surgical reattachment (Cofield, 1985).

The basic anatomical and architectural properties of the human rotator cuff muscles have been well characterized and are important for understanding the causes of injury (Bassett et al., 1990; Langenderfer et al., 2004; Veeger et al., 1991; Ward et al., 2006; Zanetti et al., 1998). Because the human glenohumeral joint has little intrinsic joint stability (O'Brien et al., 1990; Turkel et al., 1981), rotator cuff muscles and ligaments play a crucial role in maintaining stability throughout the range of motion. The tendons of the four rotator cuff muscles, while separate at the muscle bellies, come together at the glenohumeral joint and fuse with the fibrous capsule (Clark and Harryman, 1992; Sonnabend and Young, 2009). Architecturally and biomechanically, the muscles complement each other, allowing sarcomere length to vary in a way that maximizes force production over a wide range of joint angles and, therefore, maximizes stability (Ward et al., 2006). The subscapularis followed by the infraspinatus are, on average, the longest and most massive of the four muscles and are predicted to produce the greatest force based on their physiological cross-sectional areas (PCSAs). Therefore, these muscles are predicted to produce the largest compressive stabilizing forces at the glenohumeral joint. The teres minor is the least massive of the rotator cuff muscles and is predicted to produce the lowest force. The supraspinatus muscle has the shortest fibers of the rotator cuff muscles and thus operates over the greatest sarcomere length range. The supraspinatus is the site of the majority of tendon tears (Clark and Harryman, 1992; Cofield, 1985).

The rotator cuff is a relatively anatomically deep structure, and thus provides limited availability for human *in vivo* measurements. Thus, tracking tear progression has been difficult in humans, especially because tears often go unnoticed until they create a serious functional deficit (Milgrom et al., 1995). Researchers have therefore turned to animal models to study rotator cuff pathology. When making decisions about repair options, clinicians often refer to animal studies of rotator cuff injury that include mice (Thomopoulos et al., 2007), rats (Soslowsky et al., 1996), sheep (Gerber et al., 1999), rabbits (Björkenheim, 1989), dogs (Kujat, 1990), goats (Fealy et al., 2006) and others (Adams et al., 2006; Das et al., 2011; Grumet et al., 2009; MacGillivray et al., 2006; Peltz et al., 2009; Uggen et al., 2010). Although a variety of animal models have been used to study rotator cuff disease, questions remain about their relevance to humans, because of differences in their basic muscle architecture, bony anatomy and healing capacity (Brand, 2008; Dourte et al., 2010; Soslowsky et al., 1996).

It is well established that muscle architectural properties predict muscle function (Powell et al., 1984; Winters et al., 2011). Thus, differences in locomotor mode or prehensile function are likely to be manifest in muscle architecture/joint geometry differences across animals. The effects of changing locomotor pattern on bony anatomy were well highlighted in a study by Riesenfeld (Riesenfeld,

[1]Department of Bioengineering, University of California, San Diego, San Diego, CA 92093, USA. [2]Department of Radiology, University of California, San Diego, San Diego, CA 92093, USA. [3]Department of Human Evolutionary Biology, Harvard University, Cambridge, MA 02138, USA. [4]Department of Orthopaedic Surgery, University of California, San Diego, San Diego, CA 92093, USA. [5]Department of Veterans Affairs Medical Center, San Diego, CA 92093, USA.

*Author for correspondence (srward@ucsd.edu)

Received 10 December 2012; Accepted 15 September 2013

The Journal of Experimental Biology (2014) doi:10.1242/jeb.083923

List of symbols and abbreviations

ADI	architectural difference index
L_f	fiber length
L_{fn}	normalized fiber length
L_m	muscle length
L_{mn}	normalized muscle length
L_s	sarcomere length
MA	moment arm
PCSA	physiological cross-sectional area

1966). When rats were constrained to bipedal locomotion for an extended time, changes were seen in scapula size, shape and position. Scapulae of these rats became shorter and wider, and the bone rotation and infraspinous fossa surface area became more similar to those of humans than to those of control rats (Riesenfeld, 1966). These changes in bony anatomy (i.e. infraspinatus fossa depth) were likely reflections of changes in muscle function. Animals who never raise their forelimbs above their heads, for example, show differences in muscle anatomy compared with humans, who frequently do so (Bechtol, 1980; Biewener, 1990). Great structural variability can be found even among human subjects (Langenderfer et al., 2006), and thus anatomical differences among species of different size and upper extremity use patterns are expected to be much larger. These differences can impact the extent to which an animal model represents human function, disease and repair. A comparative study of animal rotator cuff muscle architecture has not been undertaken, which means that the relevance of some commonly used animal models may currently be misjudged with regard to their muscular use patterns and, therefore, muscle architectural similarity to humans. It is common to assume that animals whose size is closer to humans represent more relevant model systems.

Table 1. Architectural properties of the rotator cuff muscles across species

Muscle	Species	Mass (g)	L_{mn} (mm)	L_{fn} (mm)	L_s (μm)	Pennation angle (deg)	PCSA (cm^2)	MA (mm)
Supraspinatus	Mouse	0.03±0.00	10.93±0.20	4.18±1.16	2.38±0.03	16.92±1.12	0.07±0.00	1.07±0.05
	Rat	0.77±0.03	28.51±0.34	10.92±0.32	2.63±0.03	19.83±0.82	0.62±0.02	2.71±0.20
	Rabbit	7.89±0.61	68.85±1.54	25.21±0.85	2.42±0.11	19.58±0.67	2.80±0.23	5.67±0.14
	Dog	57.19±24.94	135.70±18.99	42.87±7.47	2.47±0.06	15.17±1.18	11.24±2.95	19.52±2.84
	Goat	142.05	226.41	65.18	1.85	17.00	19.74	26.27
	Sheep	155.28	225.33	59.44	2.10	15.25	23.87	35.51
	Pig	246.66±14.70	221.68±4.27	74.60±1.16	2.40±0.04	19.81±0.70	29.40±1.33	34.32±0.20
	Cow	1341.23	432.981	123.10	2.36	21.25	96.16	81.06
	Capuchin	7.18±1.18	43.81±4.39	16.66±1.71	3.62±0.26	16.17±0.80	3.86±0.26	7.12±0.61
	Chimpanzee	83.19	144.88	43.53	2.34	21.75	16.81	20.93
	Human	44.77±4.25	111.21±2.78	56.46±2.78	3.11±0.09	7.98±1.33	7.51±0.85	24.00
Infraspinatus	Mouse	0.03±0.00	10.24±0.31	4.02±0.29	2.48±0.02	13.83±0.67	0.07±0.01	1.04±0.02
	Rat	0.76±0.04	30.38±0.97	7.77±0.35	2.52±0.03	20.33±0.98	0.87±0.04	2.65±0.10
	Rabbit	6.26±0.30	69.67±3.42	17.77±0.57	2.45±0.18	18.42±1.04	3.18±0.24	6.43±0.06
	Dog	40.90±14.77	127.31±17.61	26.35±4.49	2.40±0.04	20.08±0.58	12.99±2.40	26.74±6.80
	Goat	137.41	265.53	36.80	2.12	26.75	31.58	19.49
	Sheep	123.42	170.16	27.29	2.38	22.50	39.57	26.81
	Pig	215.95±11.62	228.22±4.91	42.85±3.12	2.46±0.03	19.69±1.03	45.73±4.30	25.64±0.69
	Cow	1870.71	399.94	62.13	2.85	23.75	260.99	78.03
	Capuchin	8.45±1.72	66.59±0.88	18.86±0.26	2.67±0.14	29.08±12.71	3.53±0.20	7.99±0.81
	Chimpanzee	169.03	248.99	59.57	2.03	23.00	24.73	19.29
	Human	103.20±9.32	154.53±5.91	75.98±4.06	3.19±0.12	11.81±2.75	12.64±1.23	23.00
Teres minor	Mouse	0.004±0.00	7.02±0.66	2.92±0.11	2.30±0.07	15.17±0.60	0.01±0.00	1.04±0.02
	Rat	0.05±0.01	13.69±0.50	5.86±0.06	2.43±0.08	15.67±1.36	0.08±0.01	2.65±0.10
	Rabbit	0.24±0.02	25.26±1.77	8.20±2.19	2.45±0.06	10.00±0.00	0.30±0.06	6.43±0.06
	Dog	2.72±1.15	44.70±8.47	15.05±2.21	2.49±0.05	13.83±1.20	1.59±0.48	26.74±6.80
	Goat	8.81	89.32	20.27	2.66	13.50	4.00	19.49
	Sheep	8.31	76.28	17.19	3.13	16.00	4.40	26.81
	Pig	19.96±0.95	122.40±2.03	21.73±0.93	2.52±0.03	20.50±1.94	8.20±0.60	25.64
	Cow	155.32	205.37	57.09	3.07	16.50	24.70	78.03
	Capuchin	1.78±0.28	50.65±2.46	15.60±0.82	2.32±0.12	13.50±0.58	1.05±0.20	7.99±0.81
	Chimpanzee	28.95	150.81	67.16	1.86	10.50	4.01	19.29
	Human	26.10±3.02	122.01±6.20	72.45±4.03	2.95±0.11	6.81±0.93	3.52±0.45	23.00
Subscapularis	Mouse	0.04±0.01	10.86±0.09	2.79±0.04	2.32±0.04	16.44±1.18	0.14±0.05	1.04±0.02
	Rat	0.94±0.04	26.01±0.220	5.85±0.02	2.56±0.05	23.56±4.12	1.39±0.03	2.65±0.10
	Rabbit	4.61±0.21	58.09±1.784	9.90±0.79	2.36±0.06	12.33±0.51	4.40±0.59	6.43±0.06
	Dog	45.70±20.19	103.52±9.808	17.48±3.36	2.65±0.09	20.56±2.33	21.11±5.01	19.54±3.48
	Goat	66.67	221.07	23.20	2.03	16.67	26.07	25.33
	Sheep	69.98	174.55	19.48	2.24	17.00	32.53	23.93
	Pig	84.49±14.50	142.30±5.185	23.60±1.25	2.69±0.02	17.42±0.80	32.47±5.92	17.17±0.91
	Cow	1115.95	513.60	75.42	2.07	16.67	134.23	43.67
	Capuchin	16.05±2.73	68.62±2.789	17.20±0.08	2.49±0.09	15.89±0.68	8.50±1.45	6.83±0.69
	Chimpanzee	237.52	147.41	57.13	3.33	17.33	37.58	20.60
	Human	129.50±13.43	164.26±5.945	63.64±3.67	2.38±0.09	13.33±2.44	19.09±2.00	23.00

Values are means ± s.e.m. [mouse (N=3), rat (N=3), rabbit (N=3), dog (N=3), goat (N=1), sheep (N=1), pig (N=4), cow (N=1), capuchin (N=3), chimpanzee (N=1), human (N=12)]. L_{fn}, fiber lengths normalized to optimal sarcomere length of each species; L_{mn}, muscle length normalized to optimal sarcomere length of each species; L_s, sarcomere length; PCSA, physiological cross-sectional area; MA, moment arm.

The Journal of Experimental Biology (2014) doi:10.1242/jeb.083923

Another feature to consider when studying the rotator cuff is how muscle properties scale among different sized animals. Allometry is the study of size and its consequences (Gould, 1966; Schmidt-Nielsen, 1975). In this study, we are interested in how architectural parameters of muscle, such as mass, fiber length and PCSA, scale with animal size. While general scaling information is available for muscle mass and muscle architecture of lower limb muscles (Alexander et al., 1981; Biewener, 1989), scaling data specific to the rotator cuff have not been reported. This is an important gap in the literature because these data will provide the framework for hypotheses about how muscle group function changes with body mass, locomotor style or upper extremity use patterns. If one assumes that shoulder function is similar among animals, one might expect that rotator cuff muscles scale with geometric similarity, in which dimensions change proportionally with changes in organism size. This is also called isometric scaling and means that an increase in mass is associated with an increase in length proportional to $(\text{mass})^{1/3}$ and a change in area proportional to $(\text{mass})^{2/3}$ (Alexander et al., 1981). In contrast, positive allometry would indicate that a muscle architectural parameter such as muscle mass, fiber length or PCSA increases proportionally greater than body size (i.e. body mass), while negative allometry would indicate that a muscle architectural parameter increases proportionally less than body size (Alexander et al., 1981; Biewener, 1990; Eng et al., 2008; Maloiy et al., 1979). Obtaining muscle architecture scaling results for the rotator cuff in a wide variety of species ranging in body size from grams to hundreds of kilograms would allow prediction of muscle architecture based on animal mass and would allow more accurate functional comparisons to be made among muscles of different species. Because of locomotor differences and upper extremity use patterns among species, we expected to find that geometric scaling does not predict muscle architecture across all animals studied. Previous studies demonstrated scaling differences among animal groups. Animals in the family Bovidae, for example, showed consistently different scaling exponents compared to primates (Alexander et al., 1981).

While generalized scaling relationships are often discussed, complex factors play into the muscle architecture of animals of

Table 2. Relative length, PCSA and mass data for the rotator cuff muscles across species

Muscle	Species	L_{fn}/L_{mn}	L_{fn}/MA	% Total PCSA	% Total mass
Supraspinatus	Mouse	0.38±0.02	3.91±0.40	24.52±0.81	30.037±0.67
	Rat	0.38±0.02	4.07±0.21	21.08±0.12	30.41±1.05
	Rabbit	0.37±0.01	4.46±0.26	26.31±0.55	41.46±0.89
	Dog	0.31±0.02	2.20±0.19	23.64±0.73	38.48±0.90
	Goat	0.29	2.48	21.97	40.02
	Sheep	0.26	1.67	24.19	43.50
	Pig	0.34±0.02	2.17±0.05	25.55±0.90	43.57±0.95
	Cow	0.28	1.52	18.63	29.92
	Capuchin	0.38±0.01	2.35±0.20	23.18±2.48	21.57±1.17
	Chimpanzee	0.30	2.08	21.12	16.04
	Human	0.51±0.02	2.16	18.59	14.75
Infraspinatus	Mouse	0.39±0.02	3.85±0.29	23.22±0.70	26.93±0.57
	Rat	0.26±0.00	2.95±0.25	29.43±0.54	30.25±0.73
	Rabbit	0.26±0.01	2.77±0.09	29.93±1.27	32.99±0.95
	Dog	0.21±0.01	1.07±0.21	28.25±1.29	29.11±1.49
	Goat	0.14	1.49	44.57	38.71
	Sheep	0.16	1.06	38.37	34.57
	Pig	0.19±0.02	1.79±0.07	39.62±3.25	38.19±0.95
	Cow	0.16	0.80	50.57	41.73
	Capuchin	0.26±0.71	2.25±0.28	21.57±3.05	24.97±0.83
	Chimpanzee	0.28	3.61	26.61	32.59
	Human	0.49±0.02	3.14	29.89	34.00
Teres minor	Mouse	0.42±0.03	2.80±0.15	3.70±0.79	3.16±0.68
	Rat	0.43±0.01	2.22±0.11	2.54±0.15	1.93±0.12
	Rabbit	0.33±0.09	1.28±0.34	2.74±0.38	1.24±0.09
	Dog	0.34±0.04	0.60±0.07	3.28±0.48	1.84±0.15
	Goat	0.23	1.04	4.45	2.48
	Sheep	0.23	0.64	4.46	2.33
	Pig	0.18±0.01	0.84±0.03	7.14±0.58	3.56±0.28
	Cow	0.28	0.73	4.79	3.46
	Capuchin	0.31±0.01	2.01±0.31	9.29	5.35±0.13
	Chimpanzee	0.45	3.48	5.04	5.58
	Human	0.61±0.04	2.89	6.10±0.16	8.60
Subscapularis	Mouse	0.257±0.00	2.68±0.07	48.56±1.37	39.88±1.15
	Rat	0.22±0.00	2.21±0.08	46.95±0.70	37.42±0.22
	Rabbit	0.17±0.01	1.54±0.11	41.021±1.80	24.31±0.47
	Dog	0.17±0.02	0.93±0.17	44.83	30.57±0.75
	Goat	0.11	0.92	29.016	18.78
	Sheep	0.11	0.81	32.98	19.60
	Pig	0.17±0.01	1.41±0.10	27.68±3.64	14.69±1.89
	Cow	0.15	1.73	26.01	24.89
	Capuchin	0.25±0.01	2.57±0.25	49.15±1.88	48.12±0.97
	Chimpanzee	0.39	2.77	47.23	45.79
	Human	0.39±0.02	3.04	42.24	42.66

Data are means ± s.e.m.

The Journal of Experimental Biology (2014) doi:10.1242/jeb.083923

different sizes and different locomotor styles. The excursion capability of muscle is related to fiber length (Lieber and Fridén, 2000); relative fiber length would be expected to vary among species based on size and forelimb movement. Small animals such as mice, rats and rabbits, for example, move with a crouched posture (Fischer, 1994) and extend their shoulder joints through a larger range of motion during normal movement than do larger species such as sheep or cows (Biewener, 1989; McMahon, 1975). Primates move their shoulders through the widest range of motion of all species studied (Larson et al., 2001). Therefore, we predicted that fiber length and fiber length to moment arm ratios (L_{fn}/MA) would scale with negative allometry because larger species have less relative shoulder range of motion and, therefore, less relative muscle excursion demand.

Based on our understanding of animal function, we predicted the scaling effects of rotator cuff muscles. We expected muscle mass to dominate PCSA differences; therefore, we expected similar scaling relationships for muscle mass and PCSA when compared with animal mass. The supraspinatus stabilizes and abducts the glenohumeral joint and, as such, would play a much more important role in species that have less stable glenohumeral joints (greater range of motion) and abduct their forelimbs during activities of daily living, such as humans and nonhuman primates (Miller, 1932; Tuttle and Basmajian, 1978). Because the large animals do not appear to use their forelimbs in this way, relative supraspinatus muscle mass and PCSA would be smaller in these animals and we would therefore expect negative allometric scaling. Infraspinatus and teres minor provide external rotation in non-weightbearing and abduction when the leg is straight and weight-bearing. Stabilizing the glenohumeral joint against adduction during weight-bearing in straight legged, large species requires high force production. For that reason, we expected infraspinatus and teres minor to have relatively larger PCSAs in large animals and, therefore, for PCSA to scale with positive allometry among species. The subscapularis adducts and internally rotates the forelimb. These are more important functions in small animals with crouched posture and primates who internally rotate their arms (Larson and Stern, 1986) than in large, straight-legged species. Therefore, we expected subscapularis to have relatively smaller PCSAs in large animals, and therefore, scale with negative allometry among species.

A 'good' animal model of the human rotator cuff could be defined in several ways. For this study, we consider muscle architectural parameters such as PCSA, fiber length to muscle length ratio (L_{fn}/L_{mn}) and L_{fn}/MA as the most important architectural parameters. While some anatomical and architectural characteristics of various shoulder muscles of individual animals have been reported (Oxnard, 1968; Sonnabend and Young, 2009), a comprehensive architectural comparison across multiple species has not been undertaken. Therefore, this study had two aims: (1) to define the architecture of each of the four rotator cuff muscles among humans and 10 species commonly used in rotator cuff research to determine the best models for the healthy human rotator cuff, and (2) to determine how rotator cuff muscle architecture scales with body size. Based on their evolutionary similarity to humans, primates were expected to be the best models for human rotator cuffs. Because adult human forelimbs are generally not used for weight-bearing during normal locomotion, unlike any other species in the study, we expected to find that human rotator cuff muscles were smaller than would be predicted from geometric scaling relationships among quadrupeds.

RESULTS

Architectural values varied in all muscles within and among species, presumably because of animal size (Table 1). Pennation angle was similar among most species, but human muscles had lower average

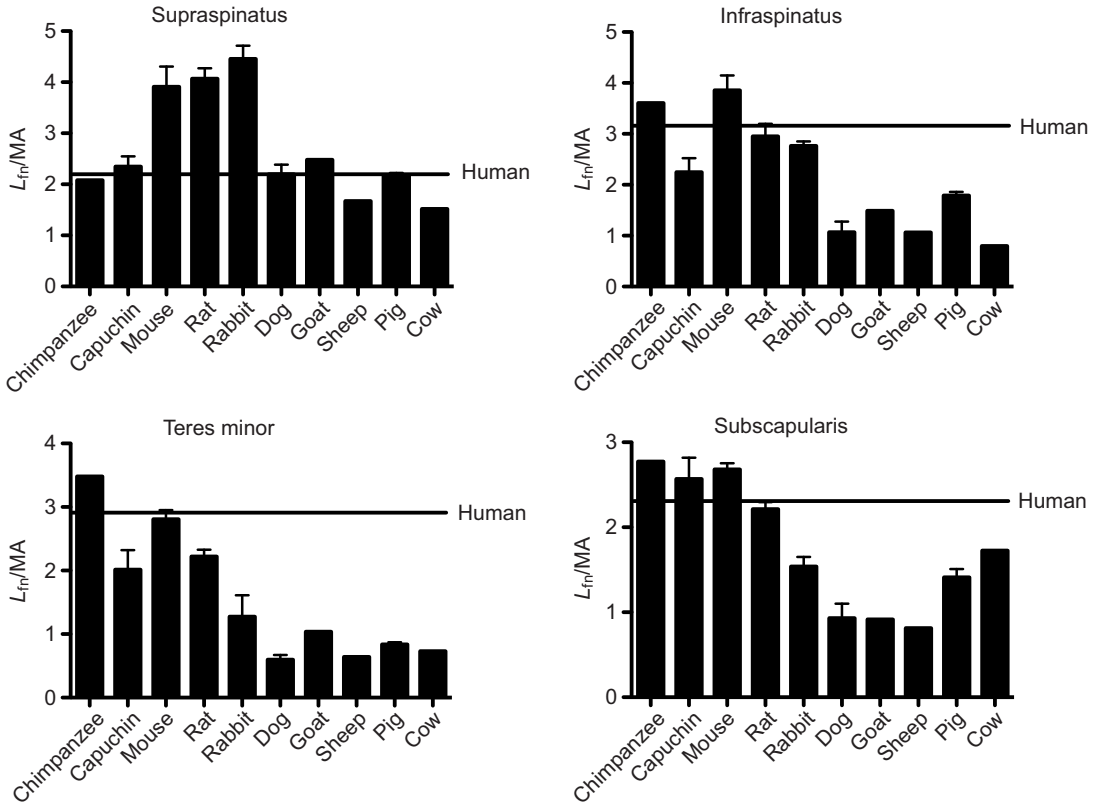

Fig. 1. Fiber length to moment arm ratio for each of the four muscles of the rotator cuff. Human data are represented by the solid line.

The Journal of Experimental Biology (2014) doi:10.1242/jeb.083923

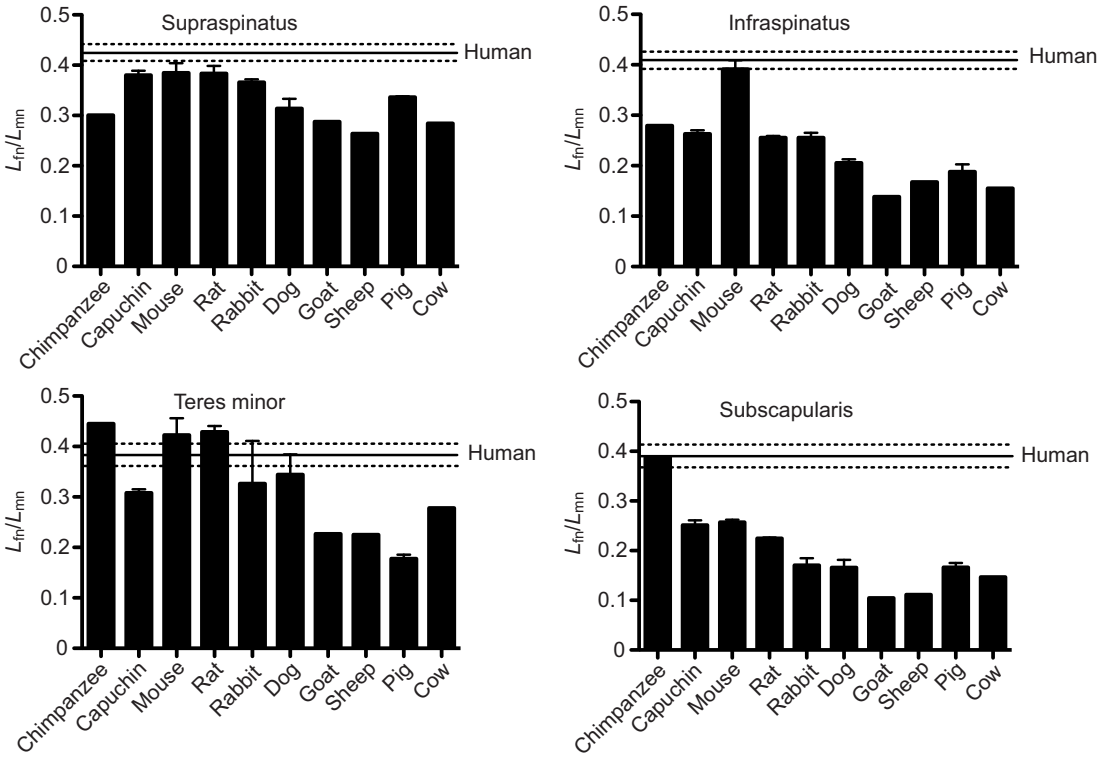

Fig. 2. Fiber length to muscle length ratio for each of the four muscles of the rotator cuff. Human data are represented by the solid line, with dotted lines showing s.e.m.

pennation angles compared with other species. Muscle mass varied over five orders of magnitude and PCSA over four among species. Given these mass differences, relative values for PCSA and mass were considered for clearer comparisons (Table 2). The mass percentage of individual rotator cuff muscles, relative to total rotator cuff mass, showed large differences between humans and non-primates. All muscles in the chimpanzee and capuchin had relative mass percentage values within 9% of the corresponding human muscle, while other species had a much larger relative supraspinatus mass compared with humans and correspondingly smaller teres minor and subscapularis relative masses. The infraspinatus had a similar contribution to total rotator cuff mass across all species studied, which was within 9% of the human value of ~30%.

L_{fn}/MA (Fig. 1) and L_{fn}/L_{mn} (Fig. 2) provide insights into muscle excursion, an important active property of the muscle (Hoy et al., 1990; Zajac, 1989). For both measurements, in all muscles except the supraspinatus, primates showed the greatest similarity to humans, followed by the small quadrupeds: mice, rats and rabbits. For the supraspinatus L_{fn}/MA ratio, humans and the other primates were more similar to pigs, dogs and goats (Table 2).

While muscle PCSA varied among species, there were similarities in an individual muscle's PCSA contribution to total rotator cuff PCSA between some species (Fig. 3). The chimpanzee had the greatest overall similarity to humans, with all PCSA percentages being within 4% of total PCSA of the corresponding human values. The capuchin, however, had values varying by as much as 9% of total PCSA from human values for several muscles. In the dog, rat, mouse and rabbit models, the subscapularis had the largest PCSA, contributing 45%, 47%, 48% and 41%, respectively, to total rotator cuff PCSA, which is comparable to the human subscapularis, which

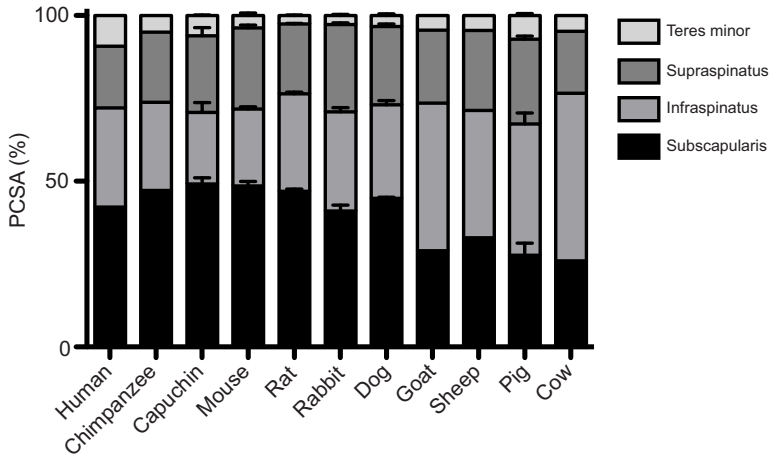

Fig. 3. Percent contribution of each muscle to total rotator cuff physiological cross-sectional area (PCSA): supraspinatus, infraspinatus, teres minor and subscapularis.

The Journal of Experimental Biology (2014) doi:10.1242/jeb.083923

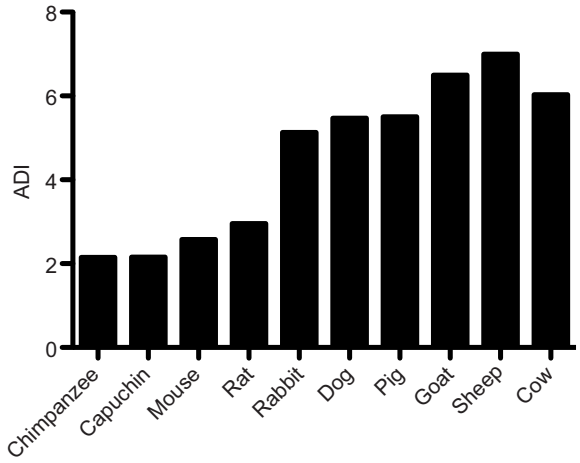

Fig. 4. Combined architectural difference index (ADI) for all rotator cuff muscles. A perfect architectural match is an ADI of zero, so low values indicate greater similarity to humans. Humans are used as comparison, and therefore have no ADI (human ADI=0).

contributed 42%. Other rotator cuff muscles for these species also shared similar percentages to human rotator cuff muscles. The goat, sheep, pig and cow percentages were similar to each other, with the infraspinatus having the largest percentage of the total rotator cuff PCSA at 39%, 40%, 39% and 50%, respectively, of total rotator cuff PCSA, but were less similar to humans relative to the smaller quadrupeds. Among species, the most variation occurred in the relative PCSA of the infraspinatus and subscapularis. Values for the teres minor and supraspinatus were similar across species.

Based on the ADI for all muscles relative to humans, chimpanzees and capuchins were found to be the closest, followed by small rodents (Fig. 4). Sheep showed the greatest difference from humans, with an ADI more than three times that of the chimpanzee, the species most architecturally similar to humans. The similarity to humans varied among individual muscles for all species (Fig. 5), but the subscapularis showed the highest similarity to humans among primates and small mammals, and the teres minor showed the lowest similarity for those species. Large mammals were less similar to humans in all muscles except the supraspinatus, where they showed values similar to those of the smaller mammals.

Log-transformed data revealed that mass, normalized fiber length (L_{fn}) and PCSA were highly correlated with body mass ($0.94 \leq r^2 \leq 1.0$; Figs 6–8, Table 3). Scaling exponents were consistent with geometric scaling relationships as determined by the mean and 95% confidence intervals. However, phylogenetic correction makes the accuracy of confidence intervals debatable. For muscle mass, exponents ranged from 0.95 to 1.06 (compared with an expected value of 1 for geometric scaling), PCSA exponents ranged from 0.59 to 0.73 (0.67 for geometric), and L_{fn} exponents ranged from 0.32 to 0.36 (0.33 for geometric). While these values bracket the mean value for geometric scaling, some muscles show slightly negative and others slightly positive allometry, but these values are not significantly different than geometric rules. When humans were removed from regression calculations, scaling relationships did not change significantly. While geometric scaling relationships appear to be supported by the mean exponent values, the 95% confidence intervals are large enough to accommodate both positive and negative allometry (Table 3). We expected muscles of different groups of species to have distinct scaling relationships. When this was tested statistically, the only differences were for the fiber length

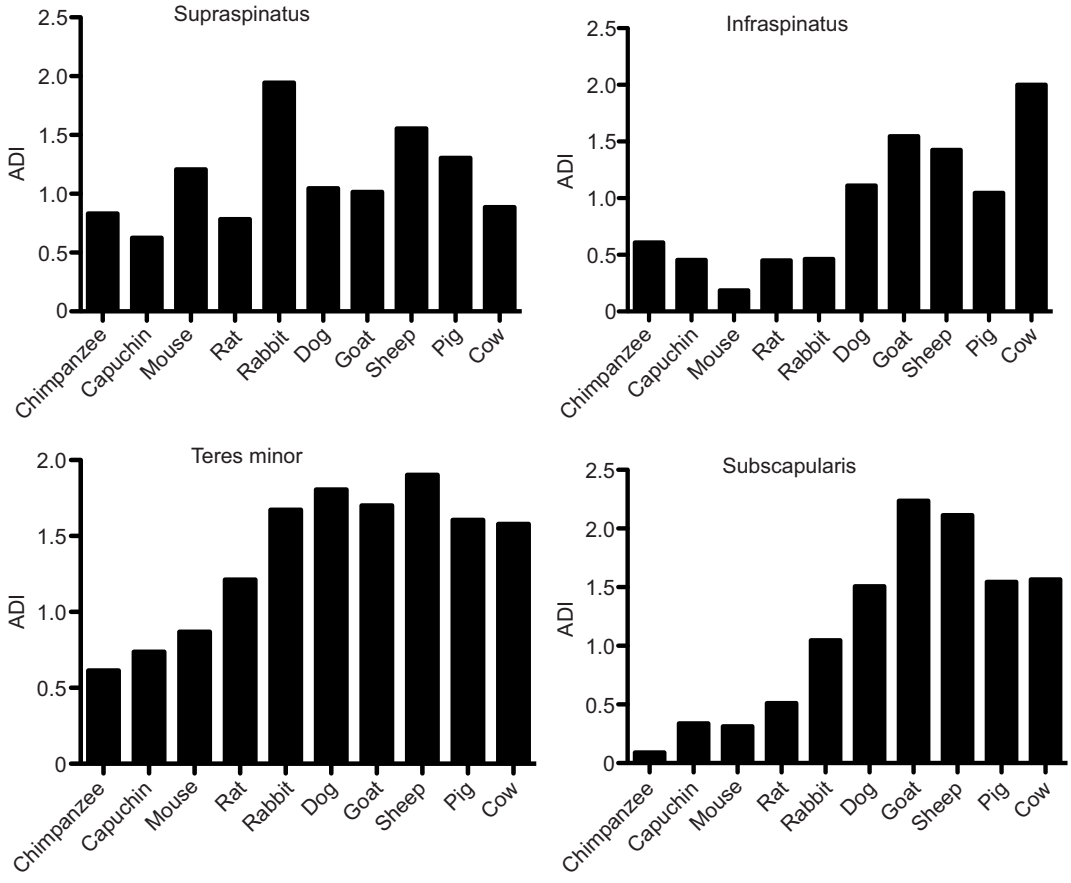

Fig. 5. Individual architectural difference index for each rotator cuff muscle.

The Journal of Experimental Biology (2014) doi:10.1242/jeb.083923

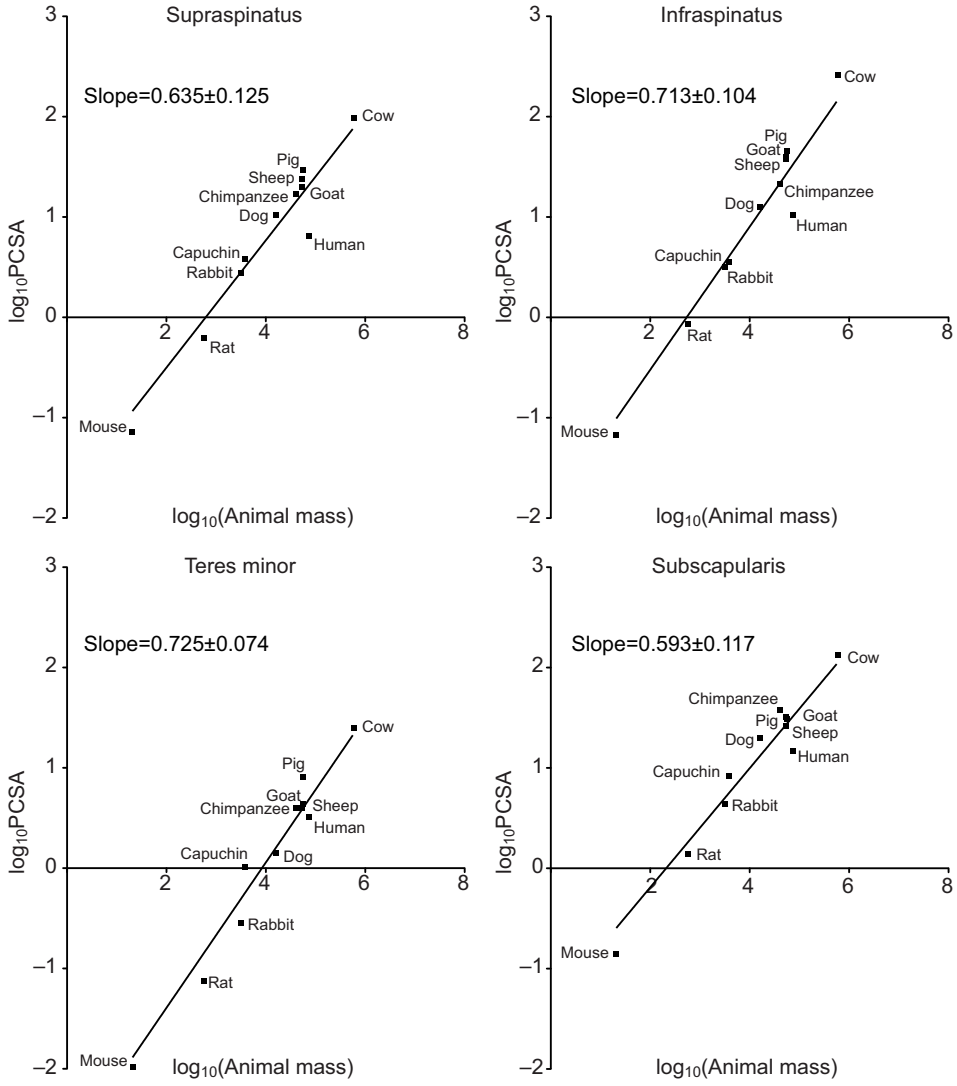

Fig. 6. Log–log plot of the relationship between PCSA and body mass. The points of the line are nearly linear, demonstrating that the scaling of PCSA percentage with respect to animal mass is geometric. Scaling is nearly geometric.

scaling relationship between the subscapularis and teres minor of small animals and large animals/primates. In the subscapularis and teres minor, small animal fiber lengths were negatively allometric (subscapularis slope=0.25±0.02, teres minor slope=0.20±0.01) while large animals were positively allometric (subscapularis slope=0.44±0.07, teres minor slope=0.39±0.05), and similarly primates were positively allometric (subscapularis slope=0.49±0.03, teres minor slope=0.53±0.11).

Clustering based on PCSA, L_{fn}/L_{mn} and L_{fn}/MA showed two distinct groups, with ungulates separated from all other species. Small animals clustered with primates rather than forming their own group. Although L_{fn}/L_{mn} and L_{fn}/MA are related to each other, removing one variable did not change the clusters. When scaling relationships were recalculated for each cluster individually, exponents remained well within the 95% confidence interval boundaries and retained values consistent with geometric scaling.

DISCUSSION

We hypothesized that, because of locomotor and upper extremity use pattern differences, rotator cuff muscle architecture and scaling relationships would differ among species. Our data suggest that, on average, muscle architecture scales geometrically with animal mass over a 20,000-fold range from ~30 g to ~600 kg. However, it is impossible to rule out positive or negative allometric scaling relationships because of the large confidence intervals obtained from our statistical analyses, similar to previous work in this area. Further exploration of our data demonstrates that ungulates appear to be ‘infraspinatus dominant’ in terms of relative rotator cuff PCSA, while the remaining species are ‘subscapularis dominant’. Within the species that are ‘subscapularis dominant’, primates are the most similar to humans.

Within the human rotator cuff muscles, the supraspinatus is the most frequently injured and its contribution to total rotator cuff PCSA is less than 20%. Within the primates studied, capuchins had the largest and humans had the smallest relative supraspinatus PCSAs. Although the observed differences between humans and non-human primates were small, the trend of decreasing relative supraspinatus mass with increasing evolutionary similarity to humans was similar to a previous report (Inman et al., 1944). This is important because it suggests that there are still upper extremity functional differences among primates that may drive muscle architectural differences. Therefore, even non-human primates, which are very similar to humans, may not represent perfect models of the human shoulder.

Because of their non-weight-bearing role, human forelimb muscles are expected to be comparatively smaller than those of

The Journal of Experimental Biology (2014) doi:10.1242/jeb.083923

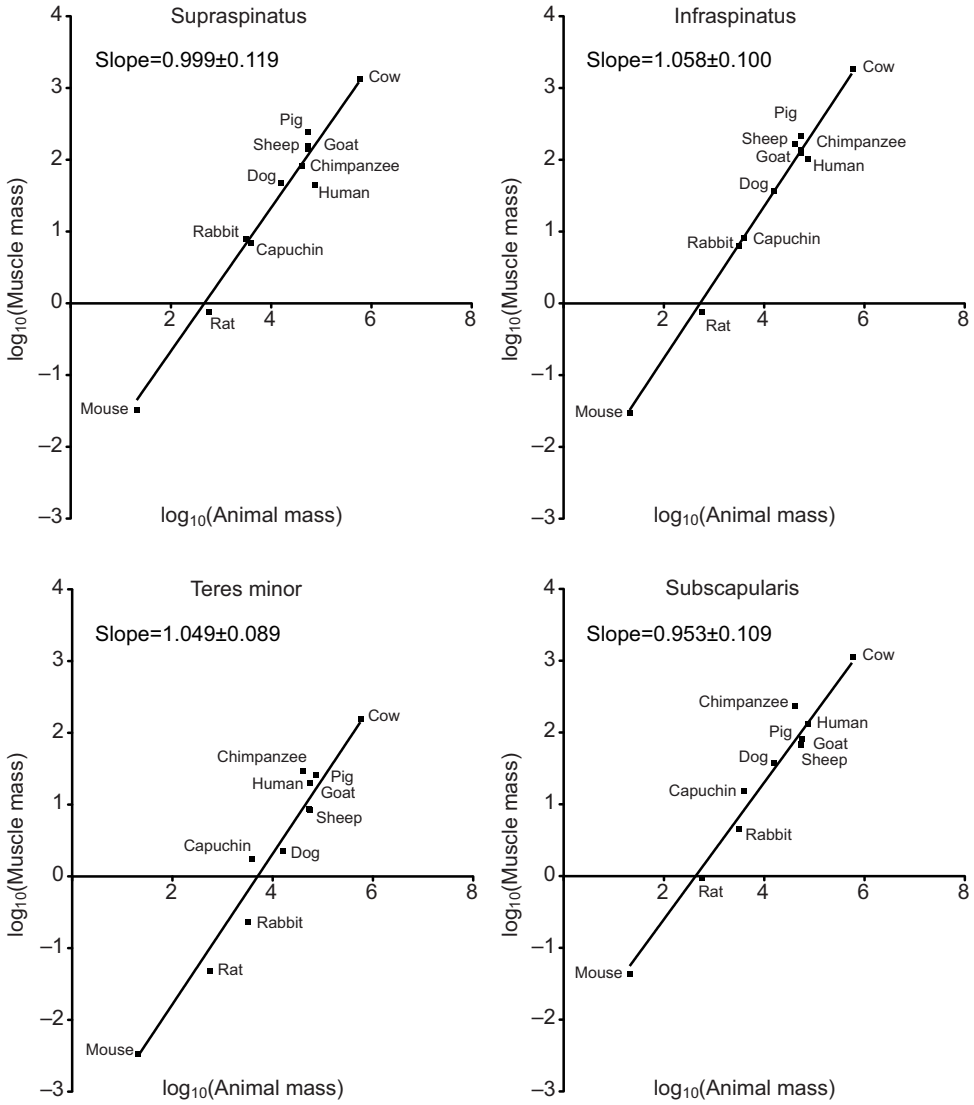

Fig. 7. Log–log plot of the relationship between muscle mass and body mass. Scaling is nearly geometric. The points of the line are nearly linear, demonstrating that the scaling of PCSA percentage with respect to animal mass is geometric.

other animal forelimbs of similar mass. This can clearly be appreciated in Fig. 9, where the human supraspinatus muscle is similar in size to that of much smaller mammals such as the capuchin or rabbit. Therefore, the effect of weight-bearing and upper extremity function on muscle size should be considered when choosing an appropriate animal model.

Non-human primates are more closely related to humans compared with non-primate mammals, and have many morphological similarities (Sonnabend and Young, 2009). Therefore, it is not surprising that the rotator cuff muscle anatomy of the two primates in this study is more similar to that of humans than the other species, because upper limb functions are more similar to those of humans. In terms of relative muscle mass contribution, chimpanzee architecture is nearly an exact match to that of the human. Although none of the non-primates are an ideal match to the absolute architectural features of the human shoulder, the relative PCSA of the rotator cuff muscles of the smaller animals such as the dog, rabbit, rat and mouse more closely matches that of the human than does the relative PCSA of the larger quadrupeds (Fig. 3). When comparing relative PCSA among muscles, primates and smaller quadrupeds are subscapularis dominant while larger ungulate quadrupeds (i.e. goat, pig, sheep and cow) are infraspinatus dominant. One possible explanation for this observation is that the weight-bearing function of rotator cuff muscles is more important in large, heavy animals that do not pronate their forelimbs, making the infraspinatus crucial for gait. Previous investigators suggested that ungulates and larger animals stand on straighter limbs than smaller species such as rodents, and their limbs pass through a smaller range of motion during movement (Biewener, 1989; Jenkins, 1971; Schmidt-Nielsen, 1984), which may also explain differences in rotator cuff musculature. In primates and smaller quadrupeds, the subscapularis may be dominant because hand positioning is important. Previous electromyographic studies in primates showed that subscapularis activation correlated with medial rotation/pronation of the forelimb and that the infraspinatus was crucial for lifting the forelimb (Larson and Stern, 1986; Tuttle and Basmajian, 1978). There may be a greater balance between these two muscles when both activities are part of daily motion. The relative PCSA of the supraspinatus and teres minor is less variable among species. Despite widely different locomotor strategies and upper extremity functions, scaling of muscle architectural properties such as fiber length and PCSA to animal mass fell within the range of geometric scaling. This has important implications in modeling, especially when primary data are not available, because architectural properties can be estimated based on body mass.

The Journal of Experimental Biology (2014) doi:10.1242/jeb.083923

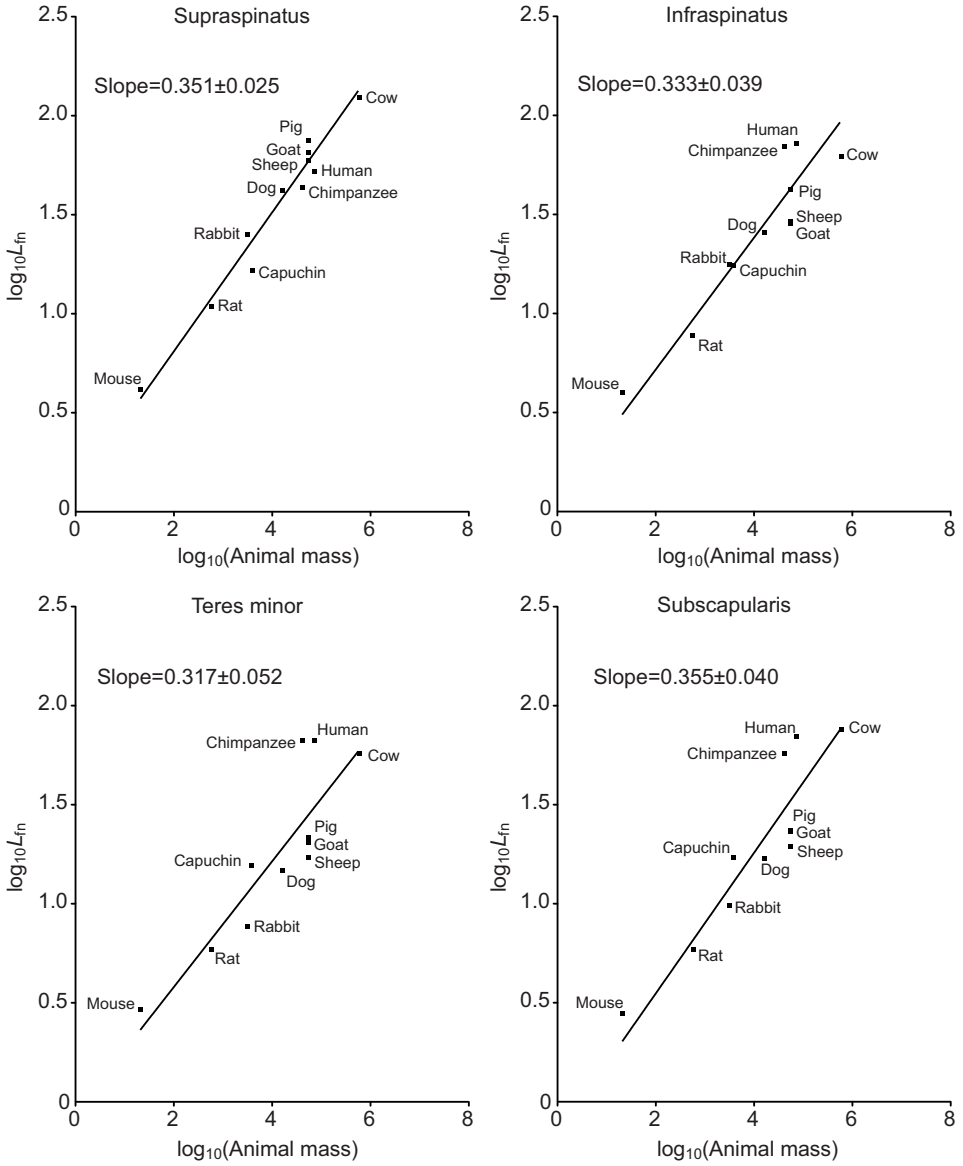

Fig. 8. Log–log plot of the relationship between normalized fiber length and body mass. Scaling is geometric with respect to animal body mass.

Previous studies comparing rotator cuff tendons found that higher primates such as humans and chimpanzees had so-called ‘true rotator cuffs’, in which the tendons of the supraspinatus, infraspinatus and teres minor muscles shared a common insertion site. Other quadrupeds such as sheep, pigs, cows, rats and mice had tendons that inserted independently (Sonnabend and Young, 2009). This difference is most likely due to the fact that humans and the other primates in the study have a much wider range of forelimb motion, and perhaps less bony stability, compared with the other animals studied and that they lift their forelimbs above their heads in the course of normal motion. In a previous study of forelimb range of motion during normal locomotion, primates had more than double the excursion of ungulates and significantly more than carnivores and rodents (Larson et al., 2001).

While geometric scaling predicts that the L_{fn}/MA ratio does not change with size, there is a nearly fourfold difference in the L_{fn}/MA ratio between large and small mammals, which likely reflects variation in locomotor demands placed upon the two groups of animals. A low L_{fn}/MA ratio shifts the balance between force production and velocity toward higher forces and lower velocities in the muscle (Lieber, 1997). Larger animals had low ratios, which suggested a need for high forces to move and stabilize their much

Table 3. Regression exponents and coefficients of the scaling equation $y=aM^b$ for muscle mass, L_{fn} and PCSA relative to body mass

	Muscle mass				PCSA				L_{fn}			
Muscle	*b*	95% CI of *b*	*r*	*a*	*b*	95% CI of *b*	*r*	*a*	*b*	95% CI of *b*	*r*	*a*
Supraspinatus	1.00±0.12	0.73–1.27	0.99	–2.67±0.50	0.64±0.13	0.35–0.92	0.99	–1.77±0.52	0.35±0.03	0.29–0.41	0.99	0.11±0.11
Infraspinatus	1.06±0.10	0.83–1.28	0.97	–2.88±0.42	0.71±0.10	0.48–0.95	0.99	–1.95±0.44	0.33±0.04	0.25–0.42	1.00	0.05±0.16
Teres minor	1.05±0.09	0.85–1.25	0.94	–3.88±0.37	0.73±0.07	0.56–0.89	0.99	–2.84±0.31	0.32±0.05	0.20–0.44	0.99	–0.06±0.22
Subscapularis	0.95±0.11	0.71–1.20	0.96	–2.51±0.46	0.59±0.12	0.33–0.86	0.99	–1.38±0.49	0.36±0.04	0.26–0.45	0.99	–0.16±0.17

Data are means ± s.e.m.

The Journal of Experimental Biology (2014) doi:10.1242/jeb.083923

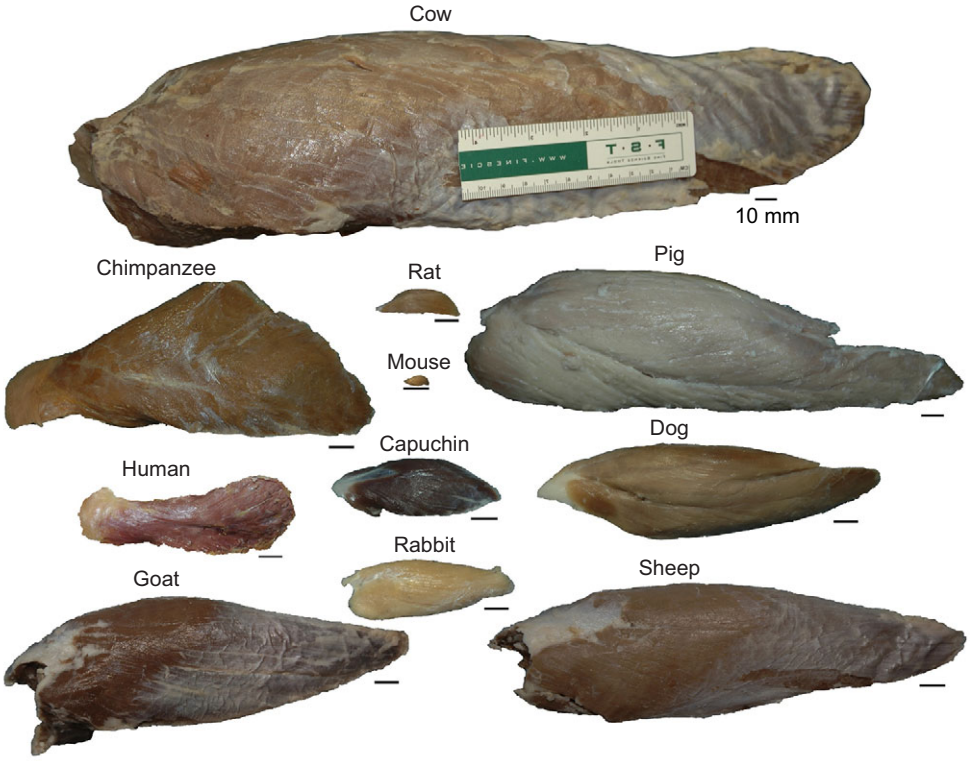

Fig. 9. Representative supraspinatus muscle from each species studied. Images are superior views with the lateral/distal end of the muscle oriented toward the left. Scale bar for all muscles is 10 mm. Average body mass for each species was: mouse=0.03 kg, rat=0.57 kg, rabbit=3.16 kg, dog=17.73 kg, goat=54.09 kg, pig=55.75 kg, sheep=54.55 kg, cow=590.91 kg, capuchin=3.97 kg, chimpanzee=40.90 kg, human=73.41 kg.

larger masses. Smaller animals such as the rat, mouse and rabbit, in contrast, showed much larger L_{fn}/MA ratios, suggesting that velocity or excursion, rather than force, is of primary importance for these prey animals. The L_{fn}/MA ratios for humans and the other two primates tended to be more similar to those of the smaller mammals. An increase in L_{fn}/MA ratio with body size is consistent with previous research (Alexander et al., 1981; Eng et al., 2008). Alexander et al. suggested that a decrease in fiber length with body size may allow larger animals to pack more fibers into the same volume to increase PCSA and, consequently, muscle force-generating capacity (Alexander et al., 1981). Larger PCSA muscles in the larger quadrupeds may contract isometrically and use long elastic tendons for elastic energy storage and recovery. This arrangement is not seen in humans because their upper limbs are not weight-bearing and thus muscle loading forces may not be sufficient to take advantage of elastic energy storage, at least in the rotator cuff. Lower L_{fn}/MA ratios in the non-human primates may be due to selective pressures related to increasing stability over economy during arboreal locomotion (Pontzer and Wrangham, 2004). In addition, it is known that intrinsic muscle speed and contractile power increase with body mass based on measurement of single fiber contraction velocities (Seow and Ford, 1991). Thus, smaller animals' muscles are specialized based on their intrinsic biochemical properties as well as their muscle-joint anatomy.

L_{fn}/L_{mn} ratios of less than 0.5 were seen in all rotator cuff muscles of all animals studied. The L_{fn}/L_{mn} ratio for smaller mammals and primates tended to be higher than that of the larger quadrupeds. Two strategies were seen for maximizing force production and producing a stable joint. One strategy was to maintain a high L_{fn}/L_{mn} ratio and thereby limit sarcomere range. Assuming constant moment arms, muscles with longer fiber lengths generate force over a narrower range of sarcomere lengths (Burkholder and Lieber, 2001; Eng et al., 2009; Lieber et al., 1997; Rome and Sosnicki, 1991; Ward et al., 2006). For all rotator cuff muscles, L_{fn}/L_{mn} ratios of humans and other primates were among the highest, meaning that these animals had the greatest potential shoulder excursion, consistent with their high L_{fn}/MA ratios. Because primates have a greater capacity for arboreality and prehension, and therefore a need for greater upper extremity mobility, a muscle design strategy shifted towards greater excursion is reasonable. A second strategy was to maintain low L_{fn}/L_{mn} ratios for force maximization over a narrower range of joint angles. In many situations, this low ratio implies that more fibers are packed in parallel, which would increase PCSA and therefore force production. In the heavier ungulates such as sheep, goats, cows and pigs, which rely on their forelimbs for weight-bearing over a limited range of motion (McMahon, 1975), lower L_{fn}/L_{mn} ratios are a reasonable strategy because the need for high force production is limited to a smaller range of joint angles.

Across all species, scaling of muscle length, muscle mass and PCSA followed geometric relationships with respect to body mass. Humans deviated slightly from the empirically determined regression line, but adding or removing humans from the analysis did not significantly change the slope of this line, suggesting that muscle dimensions increase proportionally with body size. While muscle dimensions in our study deviated slightly less from geometric similarity than in other studies, these scaling values were similar, overall, to those found in lower limbs of other mammals and birds (Alexander et al., 1981; Eng et al., 2008; Maloiy et al., 1979). It is also important to note that, while some previous studies found positive or negative allometry, they have often grouped muscles into large functional categories rather than analyzing them individually (Alexander et al., 1981). This individual treatment of muscles allows us to make scaling comments on a single structure across many animals, as was reported previously in the rat lower extremity (Eng et al., 2008).

When groups of species were compared, small animals and large animals/primates had different fiber length scaling relationships for the subscapularis and the teres minor. The small animals had a negatively allometric scaling relationship while the large animals/primates had a positively allometric scaling relationship.

The Journal of Experimental Biology (2014) doi:10.1242/jeb.083923

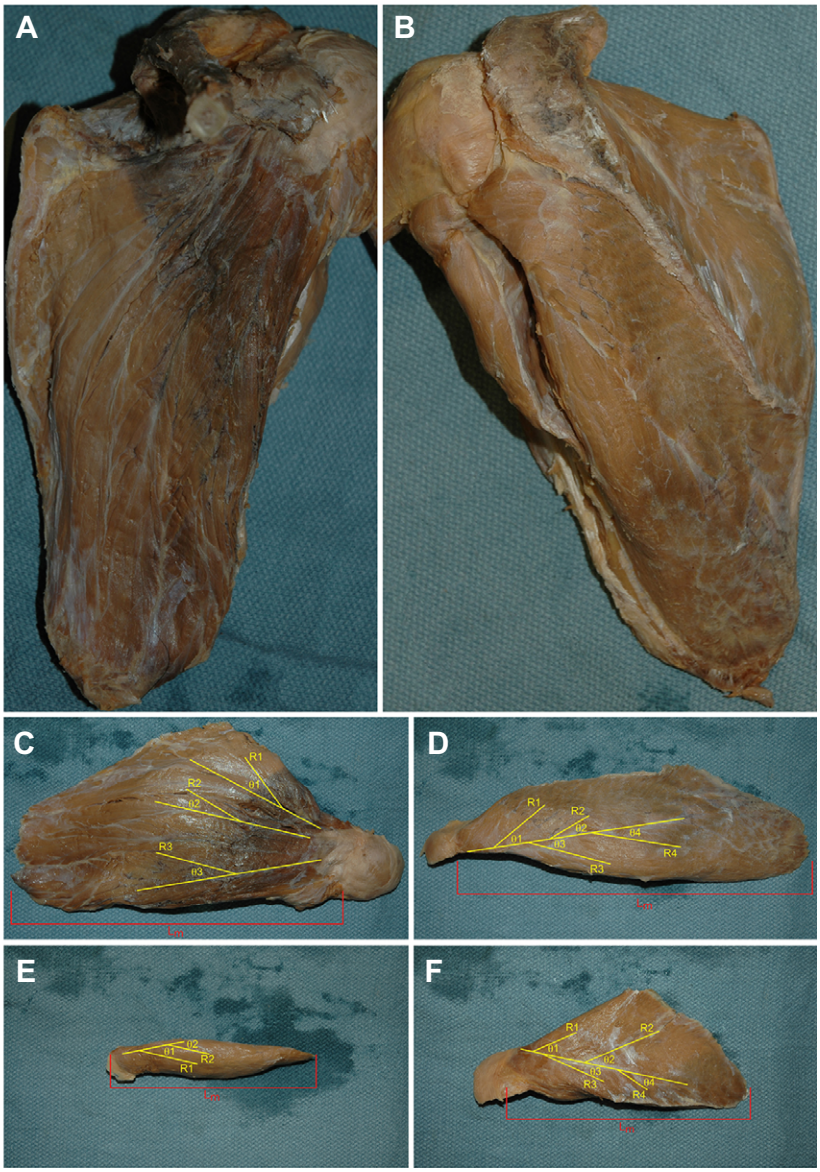

Fig. 10. Chimpanzee rotator cuff muscles. (A) Anterior and (B) posterior view of the chimpanzee scapula with musculature. Representative pennation angle measurements shown on chimpanzee shoulder muscles: (C) subscapularis, (D) infraspinatus, (E) teres minor and (F) supraspinatus.

This would suggest that the fiber length requirements in larger species are greater as a function of animal mass than in smaller animals. This was surprising to us because we expected that ungulates would have less shoulder range of motion and, therefore, shorter fibers in these muscles compared with small animals or primates. Within the small animal group, the negative fiber length allometry suggests that the most massive species in this group (rabbit) has a smaller shoulder range of motion than the smallest species in this group (mouse), meaning that the fiber length requirement for rabbit is less than for the mouse.

A limitation of this study was the very small sample size for some of the larger animals as well as the primates. An obvious future goal in this area would be to increase the sample size of each species and even add additional species, especially those with a greater range in locomotor behavior and body size, which will likely influence the scaling relationships found and provide a greater understanding of muscle scaling among species. A second limitation was the lack of published optimal sarcomere length data for some animals. A best approximation was made based on data from similar species. Third, empirical data for the teres minor moment arm was not available, but an estimate was made based on the statement by Otis et al. (Otis et al., 1994) that infraspinatus and teres minor moment arm values were similar, Finally, the results of this study are only valid for the species included in the analysis and for the loading characteristics their shoulders experience. In species for which forelimb weight-bearing is not a major form of loading (e.g. birds, fish), conclusions drawn from this study may not apply.

The use of animals in research has been crucial in furthering the understanding of human disease. A variety of animal models are widely used to study rotator cuff disease. The data presented here will be useful in selecting the appropriate animal model for future rotator cuff muscle studies. These data demonstrate that, in terms of multiple measures of muscle design such as relative PCSA and mass, as well as L_{fn}/L_{mn} and L_{fn}/MA ratios, primates and small quadrupeds are better models of the human rotator cuff than larger quadrupeds.

MATERIALS AND METHODS

Ten animals commonly used in rotator cuff research were studied: mouse (*Mus musculus*; *N*=3), Sprague-Dawley rat (*Rattus norvegicus*; *N*=3), New Zealand white rabbit (*Oryctolagus cuniculus*; *N*=3), dog (*Canis familiaris*; *N*=3), Yucatan mini-pig (*Sus scrofa*; *N*=4), sheep (*Ovis aries*; *N*=1), goat

(*Capra hircus*; *N*=1), cow (*Bos taurus*; *N*=1), chimpanzee (*Pan troglodytes*; MCZ 61068; *N*=1) and capuchin (*Cebus apella*; *N*=3). These species varied in size over a 20,000-fold range from less than 30 g (mouse) to nearly 600 kg (cow). The human data used for comparison were previously reported by our laboratory unless otherwise noted (G. C. Altobelli, C.M.E., G. D. Abrams, M.A.M., D. S. Gokhin, N. S. Fakhouri, R.L.L., A. B. Taylor and S.R.W., unpublished data). Shoulders were harvested and fixed in 10% buffered formaldehyde for 1 to 7 days, depending on size. After fixation, shoulders were stored in phosphate buffered saline. Outer layers of skin, fat and overlying muscles were removed to expose the supraspinatus, infraspinatus, teres minor and subscapularis muscles, which were identified and removed. During dissection, photographs documented general morphology and relative size (Fig. 9). Each muscle was gently blotted dry and weighed. Muscle length (L_m) was measured from the origin of the most proximal fibers to the insertion of the most distal fibers.

Multiple regions of each muscle were identified based on visual differences in pennation angle and fiber length, and these regions were consistent across species. Muscle fiber bundles were dissected from multiple predetermined regions. (Exemplar pennation angle regions are shown in Fig. 10.) While surface and deep pennation angles may not correspond perfectly, little is known about the differences between these measurements or their functional consequences. Therefore, we have measured and presented surface pennation angles to be consistent with previous literature (Powell et al., 1984). Fiber length (L_f) was measured from these bundles using calipers (0.01 mm accuracy). Under a dissecting microscope, smaller bundles were microdissected and mounted on a slide for sarcomere length (L_s) determination laser diffraction, as previously described (Lieber et al., 1990). A standard goniometer was used to measure regional surface pennation angle by measuring the angle between fibers in each region and the internal muscle tendon (Fig. 10). Values for sarcomere number (S_n) and normalized fiber length (L_{fn}) were then calculated for the isolated bundles according to the following equations:

$$S_n = \frac{L_f}{L_s}, \quad (1)$$

and

$$L_{fn} = L_f\left(\frac{L_{so}}{L_s}\right), \quad (2)$$

where L_{so} represents optimal sarcomere length for each particular species, obtained from the literature where available or estimated based on values from similar species (Bang et al., 2006; Burkholder and Lieber, 2001; Ringkob et al., 2004). Normalized muscle length (L_{mn}) was derived similarly to normalized muscle fiber length. L_{fn}/L_{mn} was calculated by dividing normalized fiber length by normalized muscle length. Physiological cross-sectional area (PCSA; cm^2) was calculated according to the following equation (Powell et al., 1984):

$$\mathrm{PCSA} = \frac{M \cdot \cos\theta}{\rho \cdot L_{fn}}, \quad (3)$$

where M is muscle mass (g), θ is pennation angle and ρ is muscle density (1.056 g cm^{-3}) (Ward and Lieber, 2005).

Muscle moment arms were measured using coronal and axial MRI plane images. The axial view was used to measure the moment arm of the supraspinatus using ImageJ software (Abramoff et al., 2004). A line was drawn to represent the line of action of the muscle's tendon. A second line, drawn perpendicularly from the initial line to the center of the humeral head, was used to represent the muscle moment arm. Moment arms for the infraspinatus, teres minor and subscapularis were measured similarly using axial view images. Human moment arm data were taken from a previously published study that used similar methods (Juul-Kristensen et al., 2000).

To compare the overall architectural similarity between humans and each of the other animal species, the architectural difference index (ADI) was calculated (Lieber and Brown, 1992). The ADI is a measure of how similar one species is to another, with a smaller ADI indicating greater similarity to humans for the parameters studied. Because functional considerations are of the most interest when choosing a rotator cuff model, fiber length-to-muscle length ratio, fiber length-to-moment arm ratio and PCSA percent were chosen as the parameters to be compared. The ADI calculation equation was previously described (Lieber and Brown, 1992):

$$\delta_{i,j} = \sqrt{\sum_{k=1}^{n}\left(\frac{P_{i,k} - P_{j,k}}{P_{\max,k} - P_{\min,k}}\right)^2}, \quad (4)$$

where n is the number of discriminating parameters (n=3), $P_{i,k}$ and $P_{j,k}$ represent the kth discriminating parameter for muscles i and j, respectively, and $P_{\max,k}$ and $P_{\min,k}$ are the maximum and minimum values for that parameter across the whole data set, respectively. Because the ADI for each animal was calculated with respect to humans, there is no ADI for humans (as the value would be 0).

Scaling equations were obtained using standard least-squares regression of $\log_{10}$-transformed variables with humans included in the calculation. Body mass was assigned as the independent variable, and means for each species were used to calculate regressions. To correct for phylogenetic distance between species, a correction was applied using the 'nlme' computation package (Pinheiro et al., 2012) in R (R Development Core Team, 2012). Data from dos Reis et al. were used for the phylogenetic tree (dos Reis et al., 2012) (supplementary material Fig. S1). The equations are reported in the form $y=aM^b$ (where y is the architectural variable, a is the scaling coefficient, M is the animal mass and b is the scaling exponent). The scaling exponent (b) is the variable used to interpret scaling relationships for each architectural variable.

To determine architectural groups, hierarchical and k-means clustering was performed with SPSS software (IBM, Armonk, NY, USA). For each species, cluster analysis included PCSA, L_{fn}/L_{mn} and L_{fn}/MA for all four rotator cuff muscles. Because of the small sample size in some species (sheep, goat, cow, chimpanzee), architectural comparisons are descriptive except when considering ADI and regression values.

Acknowledgements
Special thanks to H. Hoekstra, J. Chupasko and M. Omura from the Harvard University Museum of Comparative Zoology for facilitating access to the chimpanzee shoulder. The capuchin shoulders were provided by C. F. Ross at the University of Chicago [National Science Foundation grant BCS 0725147, PIs D. Strait and C. F. Ross]. We also appreciate the thoughtful comments of our anonymous reviewers, who helped us to substantially improve this manuscript.

Competing interests
The authors declare no competing financial interests.

Author contributions
M.A.M. performed data analysis and prepared the manuscript for submission, A.K. performed experiments and data analysis, C.M.E. performed experiments and data analysis and edited the manuscript, R.L.L. developed the approach and edited the manuscript, and S.R.W. developed the concepts and approach, supervised data collection, and edited the manuscript.

Funding
This work was supported by National Institutes of Health (NIH) grant HD050837 and a National Science Foundation Graduate Student Research Fellowship. Deposited in PMC for release after 12 months.

Supplementary material
Supplementary material available online at
http://jeb.biologists.org/lookup/suppl/doi:10.1242/jeb.083923/-/DC1

References

Abramoff, M. D., Magelhaes, P. J. and Ram, S. J. (2004). Image processing with ImageJ. *Biophotonics Int.* **11**, 36-42.
Adams, J. E., Zobitz, M. E., Reach, J. S., Jr, An, K. N. and Steinmann, S. P. (2006). Rotator cuff repair using an acellular dermal matrix graft: an *in vivo* study in a canine model. *Arthroscopy* **22**, 700-709.
Alexander, R. M., Jayes, A. S., Maloiy, G. M. O. and Wathuta, E. M. (1981). Allometry of the leg muscles of mammals. *J. Zool.* **194**, 539-552.
Bang, M.-L., Li, X., Littlefield, R., Bremner, S., Thor, A., Knowlton, K. U., Lieber, R. L. and Chen, J. (2006). Nebulin-deficient mice exhibit shorter thin filament lengths and reduced contractile function in skeletal muscle. *J. Cell Biol.* **173**, 905-916.
Bassett, R. W., Browne, A. O., Morrey, B. F. and An, K. N. (1990). Glenohumeral muscle force and moment mechanics in a position of shoulder instability. *J. Biomech.* **23**, 405-415.

Bechtol, C. O. (1980). Biomechanics of the shoulder. *Clin. Orthop. Relat. Res.* **146**, 37-41.
Biewener, A. A. (1989). Scaling body support in mammals: limb posture and muscle mechanics. *Science* **245**, 45-48.
Biewener, A. A. (1990). Biomechanics of mammalian terrestrial locomotion. *Science* **250**, 1097-1103.
Björkenheim, J. M. (1989). Structure and function of the rabbit's supraspinatus muscle after resection of its tendon. *Acta Orthop. Scand.* **60**, 461-463.
Blevins, F. T. (1997). Rotator cuff pathology in athletes. *Sports Med.* **24**, 205-220.
Brand, R. (2008). Origin and comparative anatomy of the pectoral limb. *Clin. Orthop. Relat. Res.* **466**, 531-542.
Burkholder, T. J. and Lieber, R. L. (2001). Sarcomere length operating range of vertebrate muscles during movement. *J. Exp. Biol.* **204**, 1529-1536.
Clark, J. M. and Harryman, D. T., 2nd (1992). Tendons, ligaments, and capsule of the rotator cuff. Gross and microscopic anatomy. *J. Bone Joint Surg. Am.* **74**, 713-725.
Cofield, R. H. (1985). Rotator cuff disease of the shoulder. *J. Bone Joint Surg. Am.* **67**, 974-979.
Das, R., Rich, J., Kim, H. M., McAlinden, A. and Thomopoulos, S. (2011). Effects of botulinum toxin-induced paralysis on postnatal development of the supraspinatus muscle. *J. Orthop. Res.* **29**, 281-288.
dos Reis, M., Inoue, J., Hasegawa, M., Asher, R. J., Donoghue, P. C. J. and Yang, Z. (2012). Phylogenomic datasets provide both precision and accuracy in estimating the timescale of placental mammal phylogeny. *Proc. Biol. Sci.* **279**, 3491-3500.
Dourte, L., Perry, S., Getz, C. and Soslowsky, L. (2010). Tendon properties remain altered in a chronic rat rotator cuff model. *Clin. Orthop. Relat. Res.* **468**, 1485-1492.
Eng, C. M., Smallwood, L. H., Rainiero, M. P., Lahey, M., Ward, S. R. and Lieber, R. L. (2008). Scaling of muscle architecture and fiber types in the rat hindlimb. *J. Exp. Biol.* **211**, 2336-2345.
Eng, C. M., Ward, S. R., Vinyard, C. J. and Taylor, A. B. (2009). The morphology of the masticatory apparatus facilitates muscle force production at wide jaw gapes in tree-gouging common marmosets (*Callithrix jacchus*). *J. Exp. Biol.* **212**, 4040-4055.
Fealy, S., Rodeo, S. A., MacGillivray, J. D., Nixon, A. J., Adler, R. S. and Warren, R. F. (2006). Biomechanical evaluation of the relation between number of suture anchors and strength of the bone-tendon interface in a goat rotator cuff model. *Arthroscopy* **22**, 595-602.
Fischer, M. S. (1994). Crouched posture and high fulcrum, a principle in the locomotion of small mammals: the example of the rock hyrax (*Procavia capensis*) (Mammalia: Hyracoidea). *J. Hum. Evol.* **26**, 501-524.
Gerber, C., Schneeberger, A. G., Perren, S. M. and Nyffeler, R. W. (1999). Experimental rotator cuff repair. A preliminary study. *J. Bone Joint Surg. Am.* **81**, 1281-1290.
Gould, S. J. (1966). Allometry and size in ontogeny and phylogeny. *Biol. Rev. Camb. Philos. Soc.* **41**, 587-640.
Grumet, R. C., Hadley, S., Diltz, M. V., Lee, T. Q. and Gupta, R. (2009). Development of a new model for rotator cuff pathology: the rabbit subscapularis muscle. *Acta Orthop.* **80**, 97-103.
Hoy, M. G., Zajac, F. E. and Gordon, M. E. (1990). A musculoskeletal model of the human lower extremity: the effect of muscle, tendon, and moment arm on the moment-angle relationship of musculotendon actuators at the hip, knee, and ankle. *J. Biomech.* **23**, 157-169.
Inman, V. T., Saunders, J. B. D. and Abbott, L. C. (1944). Observations on the function of the shoulder joint. *J. Bone Joint Surg.* **26**, 1-30.
Jenkins, F. A. (1971). Limb posture and locomotion in the Virginia opossum (*Didelphis marsupialis*) and in other non-cursorial mammals. *J. Zool.* **165**, 303-315.
Juul-Kristensen, B., Bojsen-Moller, F., Finsen, L., Eriksson, J., Johansson, G., Ståhlberg, F. and Ekdahl, C. (2000). Muscle sizes and moment arms of rotator cuff muscles determined by magnetic resonance imaging. *Cells Tissues Organs* **167**, 214-222.
Kujat, R. (1990). The microangiographic pattern of the rotator cuff of the dog. *Arch. Orthop. Trauma Surg.* **109**, 68-71.
Langenderfer, J., Jerabek, S. A., Thangamani, V. B., Kuhn, J. E. and Hughes, R. E. (2004). Musculoskeletal parameters of muscles crossing the shoulder and elbow and the effect of sarcomere length sample size on estimation of optimal muscle length. *Clin. Biomech.* **19**, 664-670.
Langenderfer, J. E., Carpenter, J. E., Johnson, M. E., An, K. N. and Hughes, R. E. (2006). A probabilistic model of glenohumeral external rotation strength for healthy normals and rotator cuff tear cases. *Ann. Biomed. Eng.* **34**, 465-476.
Larson, S. G. and Stern, J. T., Jr (1986). EMG of scapulohumeral muscles in the chimpanzee during reaching and 'arboreal' locomotion. *Am. J. Anat.* **176**, 171-190.
Larson, S. G., Schmitt, D., Lemelin, P. and Hamrick, M. (2001). Limb excursion during quadrupedal walking: how do primates compare to other mammals? *J. Zool.* **255**, 353-365.
Lieber, R. L. (1997). Muscle fiber length and moment arm coordination during dorsi- and plantarflexion in the mouse hindlimb. *Acta Anat.* **159**, 84-89.
Lieber, R. L. and Brown, C. G. (1992). Quantitative method for comparison of skeletal muscle architectural properties. *J. Biomech.* **25**, 557-560.
Lieber, R. L. and Fridén, J. (2000). Functional and clinical significance of skeletal muscle architecture. *Muscle Nerve* **23**, 1647-1666.
Lieber, R. L., Fazeli, B. M. and Botte, M. J. (1990). Architecture of selected wrist flexor and extensor muscles. *J. Hand Surg. Am.* **15**, 244-250.
Lieber, R. L., Ljung, B. O. and Fridén, J. (1997). Intraoperative sarcomere length measurements reveal differential design of human wrist extensor muscles. *J. Exp. Biol.* **200**, 19-25.
MacGillivray, J. D., Fealy, S., Terry, M. A., Koh, J. L., Nixon, A. J. and Warren, R. F. (2006). Biomechanical evaluation of a rotator cuff defect model augmented with a bioresorbable scaffold in goats. *J. Shoulder Elbow Surg.* **15**, 639-644.
Maloiy, G. M. O., Alexander, R. M., Njau, R. and Jayes, A. S. (1979). Allometry of the legs of running birds. *J. Zool.* **187**, 161-167.
McMahon, T. A. (1975). Using body size to understand the structural design of animals: quadrupedal locomotion. *J. Appl. Physiol.* **39**, 619-627.
Milgrom, C., Schaffler, M., Gilbert, S. and van Holsbeeck, M. (1995). Rotator-cuff changes in asymptomatic adults. The effect of age, hand dominance and gender. *J. Bone Joint Surg. Br.* **77**, 296-298.
Miller, R. A. (1932). Evolution of the pectoral girdle and fore limb in the primates. *Am. J. Phys. Anthropol.* **17**, 1-56.
O'Brien, S. J., Neves, M. C., Arnoczky, S. P., Rozbruck, S. R., Dicarlo, E. F., Warren, R. F., Schwartz, R. and Wickiewicz, T. L. (1990). The anatomy and histology of the inferior glenohumeral ligament complex of the shoulder. *Am. J. Sports Med.* **18**, 449-456.
Otis, J. C., Jiang, C. C., Wickiewicz, T. L., Peterson, M. G. E., Warren, R. F. and Santner, T. J. (1994). Changes in the moment arms of the rotator cuff and deltoid muscles with abduction and rotation. *J. Bone Joint Surg. Am.* **76**, 667-676.
Oxnard, C. E. (1968). The architecture of the shoulder in some mammals. *J. Morphol.* **126**, 249-290.
Peltz, C. D., Dourte, L. M., Kuntz, A. F., Sarver, J. J., Kim, S. Y., Williams, G. R. and Soslowsky, L. J. (2009). The effect of postoperative passive motion on rotator cuff healing in a rat model. *J. Bone Joint Surg. Am.* **91**, 2421-2429.
Pinheiro, J., Bates, D., DebRoy, S., Sarkar, D. and R Development Core Team (2012). *nlme: Linear and Nonlinear Mixed Effects Models.* R package version 3.1-105. Available at http://cran.r-project.org/web/packages/nlme/index.html.
Pontzer, H. and Wrangham, R. W. (2004). Climbing and the daily energy cost of locomotion in wild chimpanzees: implications for hominoid locomotor evolution. *J. Hum. Evol.* **46**, 315-333.
Powell, P. L., Roy, R. R., Kanim, P., Bello, M. A. and Edgerton, V. R. (1984). Predictability of skeletal muscle tension from architectural determinations in guinea pig hindlimbs. *J. Appl. Physiol.* **57**, 1715-1721.
R Development Core Team (2012). *R: A Language and Environment for Statistical Computing*. Vienna, Austria: R Foundation for Statistical Computing.
Riesenfeld, A. (1966). The effects of experimental bipedalism and upright posture in the rat and their significance for the study of human evolution. *Acta Anat.* **65**, 449-521.
Ringkob, T. P., Swartz, D. R. and Greaser, M. L. (2004). Light microscopy and image analysis of thin filament lengths utilizing dual probes on beef, chicken, and rabbit myofibrils. *J. Anim. Sci.* **82**, 1445-1453.
Rome, L. C. and Sosnicki, A. A. (1991). Myofilament overlap in swimming carp. II. Sarcomere length changes during swimming. *Am. J. Physiol.* **260**, C289-C296.
Schmidt-Nielsen, K. (1975). Scaling in biology: the consequences of size. *J. Exp. Zool.* **194**, 287-307.
Schmidt-Nielsen, K. (1984). *Scaling – Why is Animal Size So Important?* Cambridge: Cambridge University Press.
Seow, C. Y. and Ford, L. E. (1991). Shortening velocity and power output of skinned muscle fibers from mammals having a 25,000-fold range of body mass. *J. Gen. Physiol.* **97**, 541-560.
Skinner, H. B., Fitzpatrick, M. (2007). *Current Essentials Orthopedics.* McGraw-Hill Medical.
Sonnabend, D. H. and Young, A. A. (2009). Comparative anatomy of the rotator cuff. *J. Bone Joint Surg. Br.* **91**, 1632-1637.
Soslowsky, L. J., Carpenter, J. E., DeBano, C. M., Banerji, I. and Moalli, M. R. (1996). Development and use of an animal model for investigations on rotator cuff disease. *J. Shoulder Elbow Surg.* **5**, 383-392.
Thomopoulos, S., Kim, H. M., Rothermich, S. Y., Biederstadt, C., Das, R. and Galatz, L. M. (2007). Decreased muscle loading delays maturation of the tendon enthesis during postnatal development. *J. Orthop. Res.* **25**, 1154-1163.
Turkel, S. J., Panio, M. W., Marshall, J. L. and Girgis, F. G. (1981). Stabilizing mechanisms preventing anterior dislocation of the glenohumeral joint. *J. Bone Joint Surg. Am.* **63**, 1208-1217.
Tuttle, R. H. and Basmajian, J. V. (1978). Electromyography of pongid shoulder muscles II. Deltoid, rhomboid and 'rotator cuff'. *Am. J. Phys. Anthropol.* **49**, 47-56.
Uggen, C., Dines, J., McGarry, M., Grande, D., Lee, T. and Limpisvasti, O. (2010). The effect of recombinant human platelet-derived growth factor BB-coated sutures on rotator cuff healing in a sheep model. *Arthroscopy* **26**, 1456-1462.
Veeger, H. E., Van der Helm, F. C., Van der Woude, L. H., Pronk, G. M. and Rozendal, R. H. (1991). Inertia and muscle contraction parameters for musculoskeletal modelling of the shoulder mechanism. *J. Biomech.* **24**, 615-629.
Ward, S. R. and Lieber, R. L. (2005). Density and hydration of fresh and fixed human skeletal muscle. *J. Biomech.* **38**, 2317-2320.
Ward, S. R., Hentzen, E. R., Smallwood, L. H., Eastlack, R. K., Burns, K. A., Fithian, D. C., Friden, J. and Lieber, R. L. (2006). Rotator cuff muscle architecture: implications for glenohumeral stability. *Clin. Orthop. Relat. Res.* **448**, 157-163.
Winters, T. M., Takahashi, M., Lieber, R. L. and Ward, S. R. (2011). Whole muscle length-tension relationships are accurately modeled as scaled sarcomeres in rabbit hindlimb muscles. *J. Biomech.* **44**, 109-115.
Zajac, F. E. (1989). Muscle and tendon: properties, models, scaling, and application to biomechanics and motor control. *Crit. Rev. Biomed. Eng.* **17**, 359-411.
Zanetti, M., Gerber, C. and Hodler, J. (1998). Quantitative assessment of the muscles of the rotator cuff with magnetic resonance imaging. *Invest. Radiol.* **33**, 163-170.

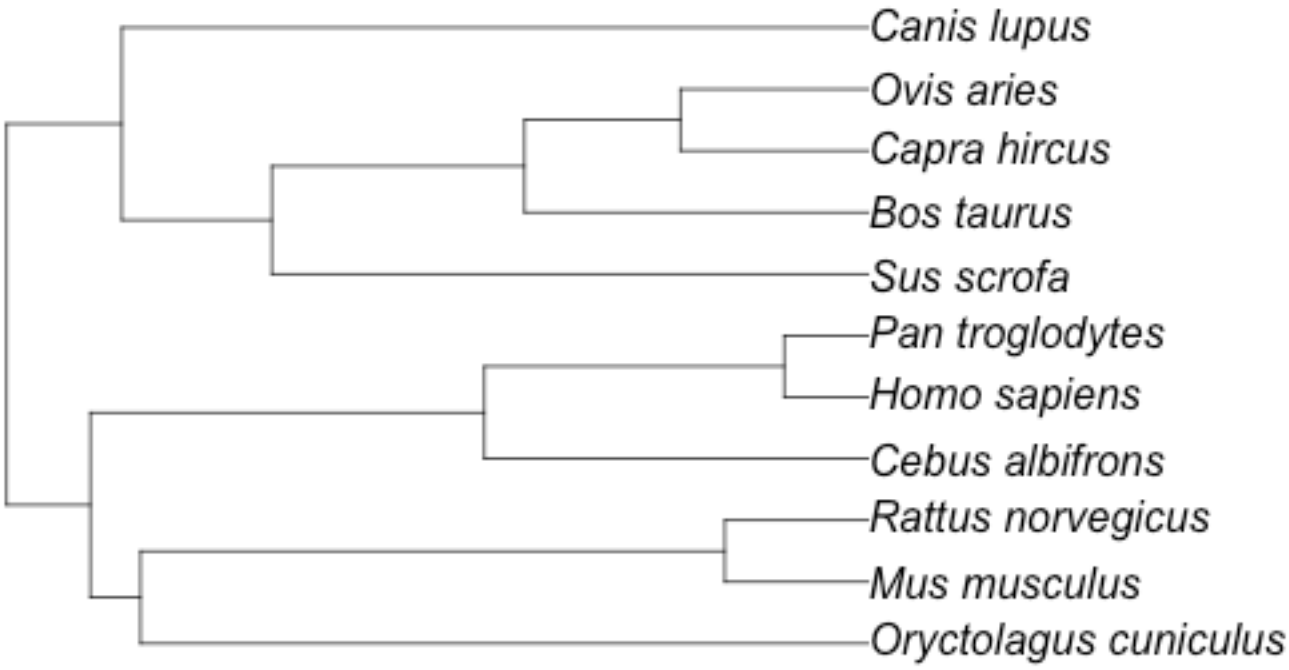

Fig. 1. Phylogenetic tree of species studied. Species are more closely related to others on the same branch of the tree (e.g. *Sus scrofa* is more closely related to *Bos taurus* than to *Canis lupus*, who is on a more distant branch of the tree). Longer branches indicate greater difference (e.g. *Ovis aries* and *Capra hircus* are less closely related than *Pan troglodytes* and *Home sapiens*). Closely related species were substituted for species that had no phylogenetic information available in the dataset used; *Canis lupus* was substituted for *Canis familiaris* and *Cebus albifrons* was substituted for *Cebus apella.*